Self-energy correction to the hyperfine splitting and the electron g factor in hydrogenlike ions

Vladimir A. Yerokhin

Max-Planck-Institut für Kernphysik, Postfach 10 39 80, D-69029 Heidelberg, Germany and Center for Advanced Studies, St. Petersburg State Polytechnical University, Polytekhnicheskaya 29, St. Petersburg RU-195251, Russia

Ulrich D. Jentschura

Department of Physics, Missouri University of Science and Technology, Rolla, Missouri 65409-0640, USA and Institut für Theoretische Physik, Universität Heidelberg, Philosophenweg 16, D-69120 Heidelberg, Germany

(Received 23 September 2009; published 8 January 2010)

The hyperfine structure (hfs) and the g factor of a bound electron are caused by external magnetic fields. For the hfs, the magnetic field is due to the nuclear spin. A uniform-in-space and constant-in-time magnetic field is used to probe the bound-electron g factor. The self-energy corrections to these effects are more difficult to evaluate than those to the Lamb shift. Here, we describe a numerical approach for both effects in the notoriously problematic regime of hydrogenlike bound systems with low nuclear charge numbers. The calculation is nonperturbative in the binding Coulomb field. Accurate numerical values for the remainder functions are provided for $2P$ states and for nS states with $n = 1, 2, 3$.

DOI: 10.1103/PhysRevA.81.012502 PACS number(s): 31.30.js, 12.20.Ds, 31.15.−p, 06.20.Jr

I. INTRODUCTION

The interaction of a bound electron and an atomic nucleus is characterized by the parameter $Z\alpha$, where Z is the nuclear charge number and α is the fine-structure constant. This universal "coupling parameter" sets the scale for calculations of the radiative corrections to various bound-state effects including the hyperfine structure (hfs) and the bound-electron g factor. Traditionally, theoretical investigations of radiative corrections in light systems relied upon an expansion in powers of $Z\alpha$ and $\ln(Z\alpha)$. However, today it is desirable to advance theory beyond the predictive limits given by the highest available terms in the $Z\alpha$ expansion. This can be done by carrying out calculations using nonperturbative (in $Z\alpha$) propagators. Such calculations demand rather sophisticated numerical techniques, which were developed relatively recently. Indeed, all-order calculations of the self-energy (SE) correction in the presence of a magnetic field started in the 1990s [1–6], extending over past years to a wide range of reference states and nuclear charge numbers [7–14].

Numerical calculations of the SE corrections are particularly difficult for low values of Z. This is mainly for two reasons. First, the goal of the calculation is the contribution beyond the known $Z\alpha$-expansion terms. For the hfs, the higher-order effects are suppressed with respect to the leading correction by a factor of $(Z\alpha)^3$. For the g factor, they enter only at order of $(Z\alpha)^5$ and thus become very small numerically in the low-Z region. Second, in actual calculations, there are additional cancellations arising at intermediate stages of the numerical procedure. These cancellations become more severe for smaller values of Z and lead to further losses of accuracy.

In this article, we treat the two most important example cases of the bound-electron SE corrections in external magnetic fields: the SE correction to the hfs and the SE correction to the bound-electron g factor. We evaluate both of these corrections for the ground and excited states of hydrogen and of light hydrogenlike ions. The first attempt at an all-order evaluation of the SE correction to the hfs of hydrogen was made in Ref. [4]. Because of insufficient numerical accuracy, the goal was reached in an indirect way: the known terms of the $Z\alpha$ expansion were subtracted from numerically determined all-order results for $Z \geqslant 5$, and the higher-order remainder was extrapolated down toward the desired value $Z = 1$. The accuracy of the numerical evaluation of the SE correction to the hfs was improved by several orders of magnitude during the past few years [8,12]. However, the precision obtained was still insufficient for a direct determination of the higher-order SE remainder at $Z = 1$, and an extrapolation procedure had to be employed again.

The studies [8,12] reported results for the higher-order contribution for the normalized difference of the $1S$ and $2S$ hfs intervals in $^3He^+$ and demonstrated a 2σ deviation of the theoretical prediction from the experimental result [15,16]. The accuracy of the extrapolation procedure of Refs. [8,12], however, has recently become a subject of some concern. In particular, an opinion was expressed in Ref. [17] that the uncertainty of the extrapolation procedure should have been estimated as four times larger than given in Refs. [8,12], which would have brought theory and experiment into agreement.

In our recent investigation [18], we performed a direct, high-precision theoretical determination of the higher-order remainder of the SE correction to the hfs of $1S$ and $2S$ states of hydrogen and light hydrogenlike ions. Good agreement was observed with the previous extrapolated values [8,12], but the accuracy was increased by several orders of magnitude. In the present paper, we report the details of this calculation and extend it to the higher excited states ($3S$, $2P_{1/2}$, and $2P_{3/2}$).

The SE correction to the bound-electron g factor is of particular importance because it is used in the determination of the electron mass value from the experimental results for the g factor of light hydrogenlike ions [19]. Already at the present level of experimental accuracy, calculations of the bound-electron g factor should be performed to all orders in $Z\alpha$. A number of all-order evaluations of the SE correction to the g factor have been accomplished [3,5,7,10,11], which resulted in an improvement in the precision of the electron mass value. However, in order to match the 10^{-12} level of accuracy anticipated in future experiments on the helium

ion [20], the precision of numerical calculations of the SE correction should be enhanced by several orders of magnitude.

The first results of our evaluation of the SE correction to the bound-electron g factor for the $1S$ state of light hydrogenlike ions were reported in Ref. [18]. In the present investigation we extend our calculation to the higher excited states ($2S$, $3S$, $2P_{1/2}$, and $2P_{3/2}$) and to a wider region of the nuclear charge number Z. Relativistic units ($\hbar = c = m = 1$) and Heaviside charge units ($\alpha = e^2/4\pi$, $e < 0$) are used throughout the paper.

Our investigations are organized as follows. In Sec. II, we discuss general formulas pertaining to the formulation of the effect within the formalism of quantum electrodynamics. We continue with a detailed description of the numerical approach in Sec. III. Numerical results are presented in Sec. IV. We conclude with a summary in Sec. V.

II. GENERAL FORMULAS

The SE correction in the presence of a binding Coulomb field and an additional perturbing potential δV is graphically represented by the Feynman diagrams shown in Fig. 1. The general expression for them can be conveniently split into three parts [21],

$$\Delta E_{\rm SE} = \Delta E_{\rm ir} + \Delta E_{\rm red} + \Delta E_{\rm ver}, \tag{1}$$

which are referred to as the irreducible, reducible, and vertex contributions, respectively.

The vertex contribution is induced by the diagram in Fig. 1(b). It can be expressed as

$$\Delta E_{\rm ver} = \frac{i}{2\pi}\int_{-\infty}^{\infty} d\omega \times \sum_{n_1 n_2} \frac{\langle n_1|\delta V|n_2\rangle\langle an_2|I(\omega)|n_1 a\rangle}{[\varepsilon_a - \omega - \varepsilon_{n_1}(1-i0)][\varepsilon_a - \omega - \varepsilon_{n_2}(1-i0)]}. \tag{2}$$

Here, I is the operator of the electron-electron interaction

$$I(\omega) = e^2 \alpha_\mu \alpha_\nu D^{\mu\nu}(\omega), \tag{3}$$

where $D^{\mu\nu}$ is the photon propagator and $\alpha^\mu = (1, \boldsymbol{\alpha})$ are the Dirac matrices. The sums over n_1 and n_2 involve both the positive-energy discrete and continuous spectra and the negative-energy continuous spectrum.

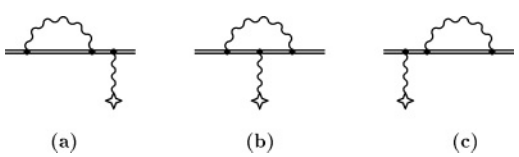

FIG. 1. Feynman diagrams representing the SE correction in the presence of an external perturbing field. The double line indicates the bound-electron propagator, which is nonperturbative in the coupling parameter $Z\alpha$ and entails an arbitrary number of Coulomb interactions with the atomic nucleus. The wavy line that ends with a cross denotes the interaction with the perturbing potential δV. The latter is given by the magnetic field of the nucleus in the case of the hfs and by a constant external magnetic field in the case of the bound-electron g factor.

The irreducible contribution is induced by a part of the diagrams in Figs. 1(a) and 1(c) that can be expressed in terms of the first-order perturbation of the reference-state wave function by δV,

$$|\delta a\rangle = \sum_{\substack{n \\ \varepsilon_n \neq \varepsilon_a}} \frac{|n\rangle\langle n|\delta V|a\rangle}{\varepsilon_a - \varepsilon_n}. \tag{4}$$

The expression for the irreducible contribution is

$$\Delta E_{\rm ir} = \langle \delta a|\gamma^0 \widetilde{\Sigma}(\varepsilon_a)|a\rangle + \langle a|\gamma^0 \widetilde{\Sigma}(\varepsilon_a)|\delta a\rangle, \tag{5}$$

where $\widetilde{\Sigma} = \Sigma - \delta m$, δm is the one-loop mass counterterm, and Σ is the one-loop SE operator,

$$\Sigma(\varepsilon, \boldsymbol{x}_1, \boldsymbol{x}_2) = 2i\alpha\,\gamma^0 \int_{-\infty}^{\infty} d\omega\, \alpha_\mu \times G(\varepsilon - \omega, \boldsymbol{x}_1, \boldsymbol{x}_2)\,\alpha_\nu D^{\mu\nu}(\omega, \boldsymbol{x}_{12}). \tag{6}$$

In the above, G denotes the Dirac Coulomb Green's function $G(\varepsilon) = [\varepsilon - \mathcal{H}(1-i0)]^{-1}$, where $\mathcal{H}$ is the Dirac Coulomb Hamiltonian, and $\boldsymbol{x}_{12} = \boldsymbol{x}_1 - \boldsymbol{x}_2$.

The reducible contribution is induced by a part of diagrams in Figs. 1(a) and 1(c) that can be expressed in terms of the first-order perturbation of the reference-state energy. It reads

$$\Delta E_{\rm red} = \delta\varepsilon_a \langle a|\gamma^0 \left.\frac{\partial}{\partial\varepsilon}\Sigma(\varepsilon)\right|_{\varepsilon=\varepsilon_a} |a\rangle, \tag{7}$$

where $\delta\varepsilon_a = \langle a|\delta V|a\rangle$.

Up to now we did not specify the particular form of the perturbing potential δV, assuming only its locality. In the following, we consider two particular choices of δV: the hfs interaction and the interaction with the magnetic field (the Zeeman effect). In the case of the hfs interaction, the perturbing potential has the form of the Fermi-Breit interaction

$$V_{\rm FB}(\boldsymbol{r}) = \frac{|e|}{4\pi}\frac{\boldsymbol{\alpha}\cdot[\boldsymbol{\mu}\times\boldsymbol{r}]}{r^3}, \tag{8}$$

(where $\boldsymbol{\mu}$ denotes the nuclear magnetic moment), and the reference-state wave function $|a\rangle$ is the wave function of the coupled system (electron+nucleus),

$$|a\rangle \to |FM_F Ij\rangle = \sum_{M_I m_a} C^{FM_F}_{IM_I j_a m_a} |IM_I\rangle|j_a m_a\rangle, \tag{9}$$

where $|IM_I\rangle$ denotes the nuclear wave function, $|j_a m_a\rangle$ is the electron wave function, F is the total momentum of the atom, and M_F is its projection. The nuclear variables can be separated out by using the standard technique of the Racah algebra. It can be demonstrated [12] that the general formulas (1)–(7) yield contributions to the hfs if one employs an electronic perturbing potential of the form

$$\delta V_{\rm hfs}(\boldsymbol{r}) = \frac{E_F}{C_{\rm hfs}}\frac{[\boldsymbol{r}\times\boldsymbol{\alpha}]_z}{r^3}, \tag{10}$$

and takes the reference-state wave function to be the electronic wave function with the momentum projection $m_a = \frac{1}{2}$,

$$|a\rangle = \left|j_a \tfrac{1}{2}\right\rangle. \tag{11}$$

In the above, E_F denotes the nonrelativistic limit of the expectation value of the Fermi-Breit operator on the reference

state, and the prefactor $C_{\rm hfs}$ is given by

$$C_{\rm hfs} = m^2(Z\alpha)^3 \frac{{\rm sgn}(\kappa_a)}{n_a^3(2\kappa_a+1)\left(\kappa_a^2-\frac{1}{4}\right)}, \tag{12}$$

where κ_a is the Dirac quantum number of the reference state and n_a is its principal quantum number.

In the case of the Zeeman splitting, the perturbing potential is

$$V_{\rm Zee}(\boldsymbol{r}) = -e\boldsymbol{\alpha}\cdot\boldsymbol{A}(\boldsymbol{r}), \tag{13}$$

where $\boldsymbol{A}(\boldsymbol{r}) = \frac{1}{2}[\boldsymbol{B}\times\boldsymbol{r}]$ is the vector potential. In practical calculations, corrections to the Zeeman splitting are conveniently expressed in terms of corrections to the g factor. It can be easily shown (see Ref. [11] for details) that the general formulas (1)–(7) yield contributions to the electronic g factor if one employs a perturbing potential of the form

$$\delta V_g(\boldsymbol{r}) = 2m[\boldsymbol{r}\times\boldsymbol{\alpha}]_z, \tag{14}$$

and the reference-state wave function with the momentum projection $m_a = 1/2$. The g-factor perturbing potential (14) differs from the hfs potential (10) only by the power of r and the prefactor.

In the following, all explicit formulas for individual contributions will be presented for the case of the hfs. When working in the coordinate representation, the corresponding formulas for the g factor can be obtained by an obvious substitution. In momentum space, the formulas for the hfs and for the g factor are different. Our present approach to the evaluation of the SE correction to the g factor closely follows the one of Ref. [11] and is therefore not described separately.

III. DETAILED ANALYSIS

A. Orientation

The general formulas presented in the previous section for individual contributions are both ultraviolet (UV) and infrared (IR) divergent. In order to obtain expressions suitable for numerical evaluation, a careful rearrangement of contributions is needed, together with a covariant regularization of divergences. The calculation of the irreducible contribution (5) can be reduced to an evaluation of a nondiagonal matrix element of the first-order SE operator (6). Its renormalization is well known and does not need to be discussed here. The numerical evaluation of the irreducible contribution was performed by a generalization of the approach of Refs. [22,23], with the use of a closed-form analytic representation of the perturbed wave function $|\delta a\rangle$ obtained in Ref. [24] (see also Ref. [25]).

The evaluation of the reducible and vertex contributions is carried out after splitting them into several parts,

$$\Delta E_{\rm red} = \Delta E^{(a)}_{\rm red} + \Delta E^{(0)}_{\rm red} + \Delta E^{(1+)}_{\rm red}, \tag{15}$$

$$\Delta E_{\rm ver} = \Delta E^{(a)}_{\rm ver} + \Delta E^{(0)}_{\rm ver} + \Delta E^{(1)}_{\rm ver} + \Delta E^{(2+)}_{\rm ver}, \tag{16}$$

where the upper index (a) labels the contributions induced by the reference-state part of the electron propagators, and the other indices specify the total number of interactions with the binding field in the electron propagators [the index $(i+)$ labels the terms generated by $\geqslant i$ such interactions].

B. Reference-state contribution

The reference-state contributions $\Delta E^{(a)}_{\rm red}$ and $\Delta E^{(a)}_{\rm ver}$ are separately IR divergent. The divergences disappear when the contributions are regularized in the same way and evaluated together. Let us now demonstrate the cancellation of the IR divergences and obtain the finite residual. The part of the vertex and reducible contributions induced by the intermediate states degenerate in energy with the reference state is

$$\begin{aligned}\Delta E^{(a)} &\equiv \Delta E^{(a)}_{\rm ver} + \Delta E^{(a)}_{\rm red} \\ &= \frac{i}{2\pi}\int_{-\infty}^{\infty} d\omega \frac{1}{(\omega - i0)^2} \\ &\quad\times\left[\sum_{\mu_{a'}\mu_{a''}} \langle a'|\delta V|a''\rangle\langle aa''|I(\omega)|a'a\rangle \right. \\ &\quad\left. - \sum_{\mu_{a'}}\langle a|\delta V|a\rangle\langle aa'|I(\omega)|a'a\rangle\right],\end{aligned} \tag{17}$$

where a is the "true" reference state and a' and a'' label the intermediate states that are degenerate with the reference state in energy and have momentum projections $\mu_{a'}$ and $\mu_{a''}$, respectively. (The intermediate states that are degenerate with the reference state in energy but of opposite parity do not induce any IR divergences because of the orthogonality of the wave functions. However, in practical calculations, we find it convenient to treat all the degenerate states on the same footing.) For simplicity, we now consider the photon propagator in the Feynman gauge. Then, the operator of the electron-electron interaction I takes the form

$$I(\omega) = \alpha\alpha_\mu\alpha^\mu D(\omega, x_{12}), \tag{18}$$

where

$$D(\omega, x_{12}) = -4\pi\int\frac{d\boldsymbol{k}}{(2\pi)^3}\frac{\exp(i\boldsymbol{k}\cdot\boldsymbol{x}_{12})}{\omega^2-\boldsymbol{k}^2-\mu^2+i0}, \tag{19}$$

with μ being the photon mass, which regularizes the IR divergences. It can be seen that all divergences in Eq. (17) originate from an integral of the form

$$J = \frac{i}{2\pi}\int_{-\infty}^{\infty} d\omega\frac{D(\omega, x_{12})}{(\omega-i0)^2}, \tag{20}$$

We now substitute Eq. (19) into the above expression, twice perform an integration by parts, evaluate the ω integral by Cauchy's theorem, and obtain

$$J = -\frac{1}{\pi}\int_0^\infty dk\frac{\cos kx_{12}}{\sqrt{k^2+\mu^2}}. \tag{21}$$

Adding and subtracting $\cos k$ in the numerator of the integrand, we separate the above expression into two parts, the first of which is convergent when $\mu\to 0$ while the other (divergent part) does not depend on x_{12}. Setting $\mu = 0$ in the convergent part and evaluating the integral, we obtain

$$J = \frac{1}{\pi}\ln x_{12} - \frac{1}{\pi}\int_0^\infty dk\frac{\cos k}{\sqrt{k^2+\mu^2}}. \tag{22}$$

The divergent part of J does not depend on the radial variables and, being substituted into Eq. (17), leads to a vanishing

contribution. We thus obtain

$$\Delta E^{(a)} = \frac{\alpha}{\pi}\left[\sum_{\mu_{a'}\mu_{a''}} \langle a'|\delta V|a''\rangle\langle aa''|\alpha_\mu\alpha^\mu \ln x_{12}|a'a\rangle - \sum_{\mu_{a'}}\langle a|\delta V|a\rangle\langle aa'|\alpha_\mu\alpha^\mu \ln x_{12}|a'a\rangle\right]. \quad (23)$$

We note that in the case when the perturbing potential δV is spherically symmetric, the reference-state contribution $\Delta E^{(a)}$ vanishes as $\langle a'|\delta V|a''\rangle = \delta_{\mu_{a''}\mu_{a'}}\langle a|\delta V|a\rangle$. In our case, however, δV represents an interaction with the magnetic field, so that $\Delta E^{(a)}$ induces a finite contribution.

In our practical calculations, the reference-state contribution was separated from the vertex and reducible parts by introducing point-by-point subtractions from the electron propagators in the integrands and was calculated separately according to Eq. (23).

C. Zero-potential parts

The zero-potential parts $\Delta E^{(0)}_{\rm red}$ and $\Delta E^{(0)}_{\rm ver}$ are separately UV divergent. They are covariantly regularized by working in an extended number of dimensions ($D = 4 - 2\epsilon$) and calculated in momentum space. The elimination of UV divergences in the sum of the reducible and vertex contributions is well documented in the literature (see, e.g., Ref. [26]), so here we operate with the *renormalized* SE and vertex operators, assuming that all UV divergences are already canceled out.

The zero-potential contribution to the reducible part is simple. It is given by

$$\Delta E^{(0)}_{\rm red} = \langle a|\delta V|a\rangle \times \int \frac{d\boldsymbol{p}}{(2\pi)^3}\overline{\psi}_a(\boldsymbol{p})\,\frac{\partial}{\partial p^0}\Sigma^{(0)}_R(p)\Big|_{p^0=\varepsilon_a}\psi_a(\boldsymbol{p}), \quad (24)$$

where $\overline{\psi} = \psi^\dagger\gamma^0$ is the Dirac adjoint. The derivative of the renormalized free SE operator $\Sigma^{(0)}_R$ can be expressed as a linear combination of three matrix structures, $\not{p} \equiv \gamma^\mu p_\mu, \gamma^0$, and the unity matrix I,

$$\frac{\partial\Sigma^{(0)}_R(p)}{\partial p^0}\Big|_{p^0=\varepsilon_a} = -\frac{\alpha}{4\pi}\left[\frac{\not{p}}{m^2}a_1(\rho) + \gamma_0 a_2(\rho) + I a_3(\rho)\right], \quad (25)$$

where $\rho = (m^2 - p^2)/m^2 = (m^2 - \varepsilon_a^2 + \boldsymbol{p}^2)/m^2$ and $a_i(\rho)$ are scalar functions, whose explicit expression is given by Eqs. (53)–(55) of Ref. [26]. Integrating over angular variables, we immediately have

$$\Delta E^{(0)}_{\rm red} = \langle a|\delta V|a\rangle\left(-\frac{\alpha}{4\pi}\right)\int_0^\infty \frac{p_r^2 dp_r}{(2\pi)^3} \times\Big\{a_1(\rho)\Big[\varepsilon_a\big(g_a^2+f_a^2\big) + 2p_r g_a f_a\Big] + a_2(\rho)\big(g_a^2+f_a^2\big) + a_3(\rho)\big(g_a^2-f_a^2\big)\Big\}, \quad (26)$$

where $p_r = |\boldsymbol{p}|$, and $g_a = g_a(p_r)$ and $f_a = f_a(p_r)$ are the upper and the lower components of the reference-state wave function in the momentum space.

The zero-potential vertex part of the SE hfs correction is induced by the hfs potential $\delta V_{\rm hfs}$ inserted in the free SE loop. The hfs potential (10) in the momentum space takes the form

$$\delta V_{\rm hfs}(\boldsymbol{q}) = \frac{E_F}{C_{\rm hfs}}(-4\pi i)\frac{[\boldsymbol{q}\times\boldsymbol{\alpha}]_z}{\boldsymbol{q}^2}. \quad (27)$$

The zero-potential vertex part is then given by

$$\Delta E^{(0)}_{\rm ver} = \frac{E_F}{C_{\rm hfs}}(-4\pi i)\int\frac{d\boldsymbol{p}_1}{(2\pi)^3}\frac{d\boldsymbol{p}_2}{(2\pi)^3} \times\overline{\psi}_a(\boldsymbol{p}_1)\frac{[\boldsymbol{q}\times\boldsymbol{\Gamma}_R(p_1,p_2)]_z}{\boldsymbol{q}^2}\psi_a(\boldsymbol{p}_2), \quad (28)$$

where $\boldsymbol{q} = \boldsymbol{p}_1 - \boldsymbol{p}_2$, p_1 and p_2 are four-vectors with the fixed time component $p_1 = (\varepsilon_a, \boldsymbol{p}_1)$ and $p_2 = (\varepsilon_a, \boldsymbol{p}_2)$, and $\boldsymbol{\Gamma}_R$ is the renormalized one-loop vertex operator. For evaluating the integrals over the angular variables in Eq. (28), it is convenient to employ the following representation of the vertex operator sandwiched between the Dirac wave functions:

$$\begin{aligned}\overline{\psi}_a(\boldsymbol{p}_1)\boldsymbol{\Gamma}_R(p_1,p_2)\psi_b(\boldsymbol{p}_2) &= \frac{\alpha}{4\pi}\big[\mathcal{R}_1\chi^\dagger_{\kappa_a\mu_a}(\hat{\boldsymbol{p}}_1)\boldsymbol{\sigma}\chi_{-\kappa_a\mu_a}(\hat{\boldsymbol{p}}_2) \\ &+\mathcal{R}_2\chi^\dagger_{-\kappa_a\mu_a}(\hat{\boldsymbol{p}}_1)\boldsymbol{\sigma}\chi_{\kappa_a\mu_a}(\hat{\boldsymbol{p}}_2) \\ &+(\mathcal{R}_3\boldsymbol{p}_1+\mathcal{R}_4\boldsymbol{p}_2)\chi^\dagger_{\kappa_a\mu_a}(\hat{\boldsymbol{p}}_1)\chi_{\kappa_a\mu_a}(\hat{\boldsymbol{p}}_2) \\ &+(\mathcal{R}_5\boldsymbol{p}_1+\mathcal{R}_6\boldsymbol{p}_2)\chi^\dagger_{-\kappa_a\mu_a}(\hat{\boldsymbol{p}}_1)\chi_{-\kappa_a\mu_a}(\hat{\boldsymbol{p}}_2)\big], \end{aligned} \quad (29)$$

where the scalar functions $\mathcal{R}_i \equiv \mathcal{R}_i(p_{1r}, p_{2r}, q_r)$ are given by Eqs. (A7)–(A12) of Ref. [26], and $\hat{\boldsymbol{p}}_i \equiv \boldsymbol{p}_i/|\boldsymbol{p}_i|$, $p_{ir} = |\boldsymbol{p}_i|$, and $q_r = |\boldsymbol{q}|$. The dependence of the integrand of Eq. (28) on the angular variables can now be parametrized in terms of the basic angular integrals K_i introduced and evaluated in the Appendix. The result is

$$\begin{aligned}\Delta E^{(0)}_{\rm ver} = \frac{E_F}{C_{\rm hfs}}\frac{\alpha}{48\pi^5}\int_0^\infty dp_{1r}\,dp_{2r}\int_{|p_{1r}-p_{2r}|}^{p_{1r}+p_{2r}} dq_r\,\frac{p_{1r}p_{2r}}{q_r} &\times\{[-p_{1r}K_1(\kappa_a)+p_{2r}K_1'(\kappa_a)]\mathcal{R}_1 \\ &+[-p_{1r}K_1(-\kappa_a)+p_{2r}K_1'(-\kappa_a)]\mathcal{R}_2 \\ &-p_{1r}p_{2r}K_2(\kappa_a)(\mathcal{R}_3+\mathcal{R}_4) \\ &-p_{1r}p_{2r}K_2(-\kappa_a)(\mathcal{R}_5+\mathcal{R}_6)\}. \end{aligned} \quad (30)$$

The above equation was used for the numerical evaluation. It contains four integrations (the fourth one, over the Feynman parameter, is implicit in the definition of the functions $\mathcal{R}_i$). All the integrations were performed using Gauss-Legendre quadratures, after making appropriate substitutions in the integration variables. We note that the integration variables p_{1r}, p_{2r}, and q_r resemble the well-known perimetric coordinates [27], in the sense that they weaken the (integrable) Coulomb singularity of the integrand at $q_r = 0$.

D. One-potential vertex part

The one-potential hfs vertex part $\Delta E^{(1)}_{\rm ver}$ is given by

$$\Delta E^{(1)}_{\rm ver} = \frac{E_F}{C_{\rm hfs}}8\pi i Z\alpha^2\int\frac{d\boldsymbol{p}\,d\boldsymbol{p}'\,d\boldsymbol{p}''}{(2\pi)^9}\overline{\psi}_a(\boldsymbol{p}) \times\frac{[\boldsymbol{p}''\times\boldsymbol{\Lambda}(p,p',p'')]_z}{(\boldsymbol{q}-\boldsymbol{p}'')^2\boldsymbol{p}''^2}\psi_a(\boldsymbol{p}'), \quad (31)$$

where $\boldsymbol{q} = \boldsymbol{p} - \boldsymbol{p}'$ is the total momentum transfer (final minus initial) for the electron vertex function $\boldsymbol{\Lambda}$, and the time component of the four-vectors is fixed by $p_0 = p_0' = \varepsilon_a$ and $p_0'' = 0$. The four-point vertex function Λ is given by

$$\Lambda_j(p, p', p'') = \frac{16\pi^2}{i} \int \frac{d^4k}{(2\pi)^4} \frac{1}{k^2} \times \frac{\gamma_\sigma(\not{p} - \not{k} + m)\gamma_0(\not{p} - \not{k} - \not{p}'' + m)\gamma_j(\not{p}' - \not{k} + m)\gamma^\sigma}{[(p-k)^2 - m^2][(p-k-p'')^2 - m^2][(p'-k)^2 - m^2]}. \tag{32}$$

The evaluation of $\Delta E^{(1)}_{\rm ver}$ is performed by using the standard technique for the evaluation of Feynman diagrams (for a short summary of the relevant formulas, see Appendix D of Ref. [28]). First, we use three Feynman parameters in order to join the four factors in the denominator of the integrand in Eq. (32). Denoting the numerator as $N_j(k)$, we obtain

$$\Lambda_j(p, p', p'') = \int dx\, dy\, dz\, 6x^2\, y \times \frac{16\pi^2}{i} \int \frac{d^4k}{(2\pi)^4} \frac{N_j(k)}{[(k - xb)^2 - x\Delta]^4}, \tag{33}$$

where x, y, and z are the Feynman parameters (here and below it is assumed that all integrals over the Feynman parameters extend from 0 to 1). We denote $b = (1-y)p + yp' + yzp''$, and $\Delta = xb^2 + m^2 - (1-y)p^2 - yp'^2 - yz(p''^2 + 2p' \cdot p'')$.

Next, we shift the integration variable $k \to k + xb$ and perform the integration over k. The result is

$$\Lambda_j(p, p', p'') = \int dx\, dy\, dz\, y \left[\frac{N_j(xb)}{\Delta^2} - \frac{x N^{\mu\nu}_{2,j} g_{\mu\nu}}{2\Delta}\right], \tag{34}$$

where $N_{2,j}$ is defined so that $N^{\mu\nu}_{2,j} k_\mu k_\nu$ is the quadratic in the k part of $N_j(k)$. We note that after shifting the integration variable, only even powers of k yield a nonzero contribution to the integral (i.e., the terms proportional to k_μ and $k_\mu k_\nu k_\rho$ vanish).

Next, the integration over p'' is carried out. We introduce the function Ξ_{ij} by

$$\Xi_{ij}(p, p') \equiv \int \frac{d\boldsymbol{p}''}{(2\pi)^3} \frac{p_i'' \Lambda_j(p, p', p'')}{\boldsymbol{p}''^2(\boldsymbol{q} - \boldsymbol{p}'')^2} = \int dx\, dy\, dz\, y \int \frac{d\boldsymbol{p}''}{(2\pi)^3} \frac{1}{\boldsymbol{p}''^2(\boldsymbol{q} - \boldsymbol{p}'')^2} \times \left[\frac{p_i'' N_{0,j}(p'')}{\Delta^2} - 2x \frac{p_i'' N_{2,j}(p'')}{\Delta}\right], \tag{35}$$

where $N_{0,j}(p'') \equiv N_j(xb)$ and $N_{2,j}(p'') \equiv N^{\mu\nu}_{2_j} g_{\mu\nu}/4$. The integral over $\boldsymbol{p}''$ in Eq. (35) can be expressed in terms of the Lewis integral [29]. However, we prefer to perform this integration straightforwardly by merging denominators using Feynman parametrization. In this way, we end up with an additional integration to be performed numerically, but the structure of the expressions involved becomes somewhat simpler.

Let us illustrate the further evaluation by considering the contribution induced by the first term in the square brackets in Eq. (35), which will be denoted by $\Xi_{0,ij}$. We merge the denominators by introducing two more Feynman parameters,

$$\frac{1}{\boldsymbol{p}''^2(\boldsymbol{q} - \boldsymbol{p}'')^2\Delta^2} = \int du\, dt \frac{6u^2 t}{(wyz)^2} \frac{1}{[(\boldsymbol{p}'' - u\boldsymbol{c})^2 + u\Omega]^4}, \tag{36}$$

where $w = 1 - xyz$,

$$\boldsymbol{c} = \frac{t}{w}[x(1-y)\boldsymbol{p} - (1 - xy)\boldsymbol{p}'] + (1-t)\boldsymbol{q}, \tag{37}$$

and

$$\Omega = -u\boldsymbol{c}^2 + (1-t)\boldsymbol{q}^2 + \frac{t}{wyz}\{x[(1-y)p + yp']^2 + m^2 - (1-y)p^2 - yp'^2\}. \tag{38}$$

Substituting Eq. (36) into Eq. (35) and shifting the integration variable, we get

$$\Xi_{0,ij}(p, p') = \int d_F \frac{6u^2 t}{yw^2 z^2} \int \frac{d\boldsymbol{p}''}{(2\pi)^3} \frac{M_{ij}}{(\boldsymbol{p}''^2 + u\Omega)^4}, \tag{39}$$

where $d_F \equiv dx\, dy\, dz\, du\, dt$ and

$$M_{ij} = (\boldsymbol{p}_i'' + u\boldsymbol{c}_i)N_{0,j}(\boldsymbol{p}'' + u\boldsymbol{c}) \equiv M_{0,ij} + M^k_{1,ij} p''_k + M^{kl}_{2,ij} p''_k p''_l + M^{klm}_{3,ij} p''_k p''_l p''_m + M^{klmn}_{4,ij} p''_k p''_l p''_m p''_n. \tag{40}$$

The above equation defines the M functions as the coefficients from the expanded form of the expression $(\boldsymbol{p}_i'' + u\boldsymbol{c}_i)N_{0,j}(\boldsymbol{p}'' + u\boldsymbol{c})$. Performing the integration over $\boldsymbol{p}''$ in Eq. (39), we obtain

$$\Xi_{0,ij}(p, p') = \frac{1}{32\pi} \int d_F \frac{u^2 t}{y\, w^2 z^2} \left\{\frac{3M_{0,ij}}{(u\Omega)^{5/2}} + \frac{M^{kk}_{2,ij}}{(u\Omega)^{3/2}} + \frac{M^{kkll}_{4,ij} + M^{klkl}_{4,ij} + M^{kllk}_{4,ij}}{(u\Omega)^{1/2}}\right\}. \tag{41}$$

Because Ω is linear in u, the integral over u is elementary and can be expressed in terms of logarithms. The four remaining integrations over the Feynman parameters remain to be evaluated numerically. To complete the evaluation of $\Xi_{0,ij}$, one needs to obtain explicit expressions for the numerators $M_{l,ij}$ and to bring them to the standard form. Under "the standard form" we understand a linear combination of independent matrix structures, see below. This is the most tedious part of the calculation, since the expressions involved are very lengthy. Usage of symbolic computation packages is indispensable in this case.

Having obtained an expression for Ξ_{ij}, we write the correction to the hfs as

$$\Delta E^{(1)}_{\rm ver} = \frac{E_F}{C_{\rm hfs}} 8\pi i Z\alpha^2 \int \frac{d\boldsymbol{p}\, d\boldsymbol{p}'}{(2\pi)^6} \overline{\psi}_a(\boldsymbol{p}) \times \Xi(p_r, p'_r, q_r; X_1, \ldots, X_{32})\psi_a(\boldsymbol{p}'), \tag{42}$$

where we used the notation $\Xi \equiv \epsilon_{0ij}\Xi_{ij}$ with ϵ_{ijk} denoting the Levi-Civita symbol. In Eq. (42), we indicate explicitly the dependence of Ξ on 32 basic matrix structures X_i. The main four of these are $[\boldsymbol{p} \times \boldsymbol{\gamma}]_z$, $[\boldsymbol{p}' \times \boldsymbol{\gamma}]_z$, $[\boldsymbol{p} \times \boldsymbol{p}']_z$, and $[\boldsymbol{\gamma} \times \boldsymbol{\gamma}]_z$. The rest are obtained by multiplying each of them by $\not{p}$, $\not{p}'$, $\not{p}\not{p}'$, γ^0, $\not{p}\gamma^0$, $\gamma^0\not{p}'$, and $\not{p}\gamma^0\not{p}'$.

TABLE I. Comparison of the convergence of the partial-wave expansion for the corrections $\Delta E_{\rm ver}^{(1+)}$ and $\Delta E_{\rm ver}^{(2+)}$ for the hfs of the $1S$ state of atomic hydrogen ($Z = 1$), in units $\Delta E/[\alpha/\pi E_F]$. $S(\kappa_{\rm max})$ is the sum of all partial contributions with $|\kappa| \leqslant \kappa_{\rm max}$, and the convergence is measured as $\kappa_{\rm max}$ is increased. δS is the increment. For $\Delta E_{\rm ver}^{(2+)}$, at the same value of $\kappa_{\rm max}$, the apparent convergence gives us roughly five more decimals as compared to $\Delta E_{\rm ver}^{(1+)}$.

$\kappa_{\rm max}$	$\Delta E_{\rm ver}^{(1+)}$		$\Delta E_{\rm ver}^{(2+)}$	
	δS	$S(\kappa_{\rm max})$	δS	$S(\kappa_{\rm max})$
3	1.580875	1.580875	3.36124192571	3.36124192571
7	−0.002317	1.578558	−0.00000693015	3.36123499556
15	−0.000660	1.577898	−0.00000079070	3.36123420487
30	−0.000183	1.577715	−0.00000009848	3.36123410639
60	−0.000049	1.577666	−0.00000001246	3.36123409393
120	−0.000010	1.577656	−0.00000000122	3.36123409270
Extrap.	−0.000015(15)	1.577641(15)	−0.00000000041(44)	3.36123409229(44)

In order to perform the integration over all angular variables in Eq. (42) except for $\xi = \hat{\boldsymbol{p}} \cdot \hat{\boldsymbol{p}}'$, we define the angular integrals Y_i that correspond to the basic matrices X_i by

$$\int d\hat{\boldsymbol{p}} d\hat{\boldsymbol{p}}' \overline{\psi}_a(\boldsymbol{p}) X_i F(p_r, p_r', q_r) \psi_a(\boldsymbol{p}') = \int_{-1}^{1} d\xi\, Y_i F(p_r, p_r', q_r), \quad i = 1, \ldots, 32, \tag{43}$$

where F is an arbitrary function. All Y_i may be expressed in terms of the elementary angular integrals listed in the Appendix.

Using the angular integrals Y_i, we can write the final expression for the one-potential vertex term suitable for a numerical evaluation as

$$\Delta E_{\rm ver}^{(1)} = \frac{E_F}{C_{\rm hfs}} \frac{\alpha(Z\alpha)}{6\pi^4} \int_0^\infty dp_r\, dp_r' \times \int_{|p_r - p_r'|}^{p_r + p_r'} dq_r\; p_r p_r' q_r\, \Xi(p_r, p_r', q_r; Y_1, \ldots, Y_{32}). \tag{44}$$

Altogether, Eq. (44) contains seven integrations to be performed numerically, three of them being written explicitly, and four Feynman-parameter integrations contained in the definition of the function Ξ. The numerical evaluation was performed using Gauss-Legendre quadratures for all integrations. In order to prevent losses of accuracy due to numerical cancellations, we used quadruple-precision arithmetic (accurate to roughly 32 decimals) in a small part of the code, which was identified to be numerically unstable. The evaluation was rather time consuming (about a month of processor time for each value of Z and each state) and was performed with the help of the parallel computational environment at MPI Heidelberg.

The one-potential vertex part has been crucial to our calculation, and so it may be appropriate to summarize once more the basic steps in its evaluation. First of all, let us recall that our "one-potential vertex part" actually involves two vertices inside the loop, one being a Coulomb vertex and the other being a magnetic vertex (coupling to the external field). Therefore, there are three fermion propagators inside the loop and one photon propagator, necessitating the introduction of three Feynman parameters to join denominators. The incoming Coulomb momentum and the exchanged momentum with the external field entail two further Feynman parameters, one of which is integrated out analytically. In addition to the four remaining Feynman parameters, we have two radial integrations over the absolute values of the initial ($\boldsymbol{p}'$) and final ($\boldsymbol{p}$) electron momenta and an integration over the direction cosine ξ (transformed by a change of variable to an integration over $q_r = |\boldsymbol{p} - \boldsymbol{p}'|$). The three additional integrations account for the resulting seven-dimensional integral. In the corresponding calculation in free QED, one could hope to carry out the radial integrations analytically, because the incoming and outgoing fermions are on the mass shell and described by plane waves. Here, however, the bound states are being off the mass shell and have a much more complicated structure, so the radial integrations have to be evaluated numerically. The separate calculation of the full one-potential vertex part as described in the current section leads to a numerically favorable scheme, because this part can then be subtracted from the integrand of the remaining nonperturbative vertex contribution, thereby leading to a drastic improvement in the convergence of the resulting partial-wave expansion (see Table I above).

E. Many-potential vertex part

The general expression for the many-potential vertex part $\Delta E_{\rm ver}^{(2+)}$ is obtained from Eq. (2) by applying the appropriate set of subtractions in the electron propagators. The required subtractions are given by

$$G\delta V G \to G\delta V G - G^{(a)}\delta V G^{(a)} - G^{(0)}\delta V G^{(0)} - G^{(0)}\delta V G^{(1)} - G^{(1)}\delta V G^{(0)}, \tag{45}$$

where G denotes the bound-electron propagator, $G^{(0)}$ is the free-electron propagator, $G^{(1)}$ is the electron propagator with one interaction with the binding Coulomb field, and $G^{(a)}$ is the reference-state part of the bound-electron propagator. This subtraction takes into account all terms which have been calculated separately using different approaches, as described above.

In order to perform a numerical evaluation of $\Delta E_{\rm ver}^{(2+)}$, it is convenient to rotate the integration contour of the photon energy ω from $(-\infty, \infty)$ to be parallel to the imaginary axis of the ω complex plane. In this work, we define a deformed ω integration contour C_{LH} consisting of two parts, a

low-energy part C_L and a high-energy part C_H. The low-energy part contains the interval $\omega \in (\Delta - i0, -i0)$ on the lower bank of the cut of the photon propagator and the interval $(i0, \Delta + i0)$ on the upper bank of the cut, with $\Delta = Z\alpha\varepsilon_a$. The high-energy part consists of two intervals, $(\Delta + i0, \Delta + i\infty)$ and $(\Delta - i0, \Delta - i\infty)$. The contour C_{LH} defined in this way differs from the one used by J. Mohr [30] only by the choice of the separation point Δ (the value $\Delta = \varepsilon_a$ instead of $\Delta = Z\alpha\varepsilon_a$ was employed in Ref. [30]).

The high-energy part of $\Delta E^{(2+)}_{\rm ver}$ is given by

$$\Delta E^{(2+)}_{{\rm ver},H} = -\frac{1}{\pi}{\rm Re}\int_0^\infty d\omega \times \sum_{n_1 n_2}\Bigg[\frac{\langle n_1|\delta V|n_2\rangle\langle an_2|I(\Delta+i\omega)|n_1 a\rangle}{(\varepsilon_a-\Delta-i\omega-\varepsilon_{n_1})(\varepsilon_a-\Delta-i\omega-\varepsilon_{n_2})} - ({\rm subtractions})\Bigg], \tag{46}$$

where the subtractions are given by Eq. (45). The low-energy part of $\Delta E^{(2+)}_{\rm ver}$ needs a careful treatment because of single and double poles situated near the contour C_L, which are due to virtual bound states of lower energy than the reference state. The single poles can be integrated via a Cauchy principal value prescription, and the double poles can be converted to single poles via an integration by parts. We thus write the low-energy part of $\Delta E^{(2+)}_{\rm ver}$ as

$$\Delta E^{(2+)}_{{\rm ver},L} = -\frac{1}{\pi}P\int_0^\Delta d\omega \times \Bigg[\sum_{\substack{n_1 n_2\\ {\rm not}\,0<\varepsilon_{n_1}=\varepsilon_{n_2}<\varepsilon_a}}\frac{F_{n_1n_2}(\omega)}{(\varepsilon_a-\omega-\varepsilon_{n_1})(\varepsilon_a-\omega-\varepsilon_{n_2})} - \sum_{0<\varepsilon_n<\varepsilon_a}\frac{F'_{nn}(\omega)}{\varepsilon_a-\omega-\varepsilon_n} - ({\rm subtractions})\Bigg] - \frac{1}{\pi}\sum_{0<\varepsilon_n<\varepsilon_a}\frac{F_{nn}(\Delta)}{\varepsilon_a-\Delta-\varepsilon_n}, \tag{47}$$

where

$$F_{n_1n_2}(\omega) = \langle n_1|\delta V|n_2\rangle\langle an_2|{\rm Im}\,[I(\omega)]\,|n_1 a\rangle, \tag{48}$$

the prime denotes the derivative over ω, and P denotes the Cauchy principal value of the integral. In Eq. (47), all terms that induce double poles on the interval $\omega \in (0, \Delta)$ (i.e., intermediate states with $0 < \varepsilon_{n_1} = \varepsilon_{n_2} < \varepsilon_a$) have been integrated by parts. We recall that the term with $\varepsilon_{n_1} = \varepsilon_{n_2} = \varepsilon_a$ is removed by the $G^{(a)}$ part of the subtraction (45).

The need to evaluate the principal value of the integral over ω complicates the numerical calculation of the low-energy part. In the case when there is a single pole only (which takes place for the $2s$ and $2p_{1/2}$ reference state), the problem is most easily solved by employing a numerical quadrature symmetric around the position of the pole. In the general case with more than one singularity to be treated, this approach is not effective. A better way is to introduce subtractions in the integrand that remove the singularities at the poles and to evaluate the principal value of the integral of the subtracted terms analytically. We introduce the subtractions by observing that the following difference does not have any singularities on the interval $\omega \in (0, \Delta)$,

$$\sum_{\substack{n_1 n_2\\ {\rm not}\,0<\varepsilon_{n_1}=\varepsilon_{n_2}\leqslant\varepsilon_a}}\frac{\langle n_1|\delta V|n_2\rangle\langle an_2|{\rm Im}[I(\omega)]|n_1 a\rangle}{(\varepsilon_a-\omega-\varepsilon_{n_1})(\varepsilon_a-\omega-\varepsilon_{n_2})} - \sum_{0<\varepsilon_{n_1}<\varepsilon_a}\frac{\langle a\delta n_1|{\rm Im}[I(\varepsilon_a-\varepsilon_{n_1})]|n_1 a\rangle}{\varepsilon_a-\omega-\varepsilon_{n_1}} - \sum_{0<\varepsilon_{n_2}<\varepsilon_a}\frac{\langle an_2|{\rm Im}[I(\varepsilon_a-\varepsilon_{n_2})]|\delta n_2 a\rangle}{\varepsilon_a-\omega-\varepsilon_{n_2}}, \tag{49}$$

where

$$|\delta n_1\rangle = \sum_{n_2\neq n_1}\frac{|n_2\rangle\langle n_2|\delta V|n_1\rangle}{\varepsilon_{n_1}-\varepsilon_{n_2}}. \tag{50}$$

We note that the terms with $(\varepsilon_{n_1} = \varepsilon_a,\ \varepsilon_{n_2} \neq \varepsilon_a)$ and $(\varepsilon_{n_1} \neq \varepsilon_a,\ \varepsilon_{n_2} = \varepsilon_a)$ present in Eq. (49) do not induce any singularities because ${\rm Im}[I(0)] = 0$. The perturbed wave function $|\delta n_1\rangle$ is known analytically (for the hfs perturbing potential, both the diagonal and the nondiagonal in κ parts; for the g-factor perturbing potential, only the diagonal in κ part) from the generalized virial relations for the Dirac equation [24,25].

In order to complete our discussion of the evaluation of the many-potential vertex part, we present the explicit expression for it after the integration over the angular variables. This expression reads

$$\Delta E^{(2+)}_{\rm ver} = \frac{E_F}{C_{\rm hfs}}\frac{i\alpha}{2\pi}\int_{C_{LH}}d\omega\sum_{n_1n_2L}\Bigg[\begin{Bmatrix} j_1 & j_2 & 1\\ j_a & j_a & L\end{Bmatrix} \times \frac{P(n_1,n_2)R_L(\omega, an_2n_1a)}{(\varepsilon_a-\omega-\varepsilon_{n_1})(\varepsilon_a-\omega-\varepsilon_{n_2})} - ({\rm subtractions})\Bigg], \tag{51}$$

where R_L is a relativistic generalization of the Slater radial integral, whose explicit expression is given in Ref. [32]. $P(n_1, n_2)$ is given by

$$P(n_1,n_2) = (-1)^{j_a+1/2}C^{10}_{j_a-1/2,j_a1/2} \times \frac{\kappa_1+\kappa_2}{\sqrt{3}}\langle-\kappa_2||C^{(1)}||\kappa_1\rangle R_{-2}(n_1,n_2), \tag{52}$$

where $C^{jm}_{j_1m_1,j_2m_2}$ is the Clebsch-Gordan coefficient, $C^{(l)}_m = \sqrt{4\pi/(2l+1)}Y_{lm}$ is a normalized spherical harmonic, and

$$R_{-2}(n_1,n_2) = \int_0^\infty dr[g_{n_1}(r)f_{n_2}(r) + f_{n_1}(r)g_{n_2}(r)]. \tag{53}$$

The numerical evaluation of the many-potential vertex contribution is the most difficult part of the calculation. The key feature that limits the accuracy achievable in a numerical calculation is the convergence of the partial-wave expansion. We recall that the many-potential vertex contribution $\Delta E^{(2+)}_{\rm ver}$ contains two and more Coulomb interactions (and a magnetic interaction) inside the self-energy loop. The convergence of its partial-wave expansion is much better than that for the vertex contribution with just one Coulomb interaction. In order to illustrate this point, Table I presents a comparison

of the partial-wave expansion of the vertex contribution with two and more Coulomb interactions, $\Delta E_{\rm ver}^{(2+)}$, and of that with one and more Coulomb interactions, $\Delta E_{\rm ver}^{(1+)}$. It can be seen that the subtraction of the one-potential vertex contribution improves the numerical accuracy by about five orders of magnitude.

The partial-wave expansion was cut off at the maximum value of $|\kappa_{\rm max}| = 120$. Quadruple-precision arithmetics was required for the Dirac Green's function in order to control the numerical accuracy at the required level. This computation was performed with a quadruple-precision generalization of the code for the Dirac Green's function developed in Refs. [8,32]. It should be mentioned that the evaluation of the high-energy part of $\Delta E_{\rm ver}^{(2+)}$ with the integration contour C_{LH} requires the Dirac Green's function with general complex values of the energy argument. (This is in contrast to the approach used in Refs. [22,23,30], where the integration contour is chosen in such a way that only the real and purely imaginary values of the energy argument are required.) The computation of the Dirac Green's function for general complex energies ω becomes numerically unstable when κ is large and $\arg(\omega)$ is close to $\pi/4$. Because of this, we were not able to extend the partial-wave summation beyond $|\kappa_{\rm max}| = 120$.

The general scheme of our evaluation is as follows. We perform the summation over κ directly in the integrand, before any integrations. The summation is terminated when a suitable convergence criterion is fulfilled or when the cutoff value $|\kappa_{\rm max}|$ is reached. In order to estimate the dependence of the final result on the cutoff parameter, results for several intermediate cutoffs are stored, each consequent one being twice as large as the previous one (see Table I for an illustration). The omitted tail of the expansion was estimated by using the ϵ algorithm for the Padé approximation, and the uncertainty of the extrapolation was taken to be about 50–200% of the estimated tail.

F. Many-potential reducible part

According to Eq. (7), the reducible part of the SE correction involves the derivative of the SE operator, "sandwiched" in the reference state. The zero-potential part of the reducible contribution has already been discussed in Sec. III C; it involves the derivative of the free electron propagator with respect to the reference-state energy. The reference-state contribution to the reducible part has been treated in Sec. III B, together with the reference-state contribution to the vertex term, thereby mutually canceling the IR divergence inherent to both reference-state contributions. The total reference-state contribution is summarized in Eq. (23). Left is the many-potential reducible part,

$$\Delta E_{\rm red}^{(1+)} = \langle a|\delta V|a\rangle \times \langle a|\gamma^0 \frac{\partial}{\partial\varepsilon}[\Sigma(\varepsilon) - \Sigma^{(0)}(\varepsilon) - \Sigma^{(a)}(\varepsilon)]|_{\varepsilon=\varepsilon_a}|a\rangle. \tag{54}$$

Here, $\Sigma^{(0)}(\varepsilon)$ and $\Sigma^{(a)}(\varepsilon)$ are obtained from Eq. (6) by a replacement of the full Dirac-Coulomb Green's function G by the free Green's function $G^{(0)}$ and by the reference-state part of the propagator $G^{(a)}$. For the term with $G^{(a)}$, we have

$$\Sigma^{(a)}(\varepsilon, \boldsymbol{x}_1, \boldsymbol{x}_2) = 2i\alpha\gamma^0 \int_{-\infty}^{\infty} d\omega \alpha_\mu \times G^{(a)}(\varepsilon - \omega, \boldsymbol{x}_1, \boldsymbol{x}_2)\alpha_\nu D^{\mu\nu}(\omega, \boldsymbol{x}_{12}). \tag{55}$$

In coordinate space, a representation of $G^{(a)}$ reads

$$G^{(a)}(\varepsilon - \omega, \boldsymbol{x}_1, \boldsymbol{x}_2) = \sum_{\substack{n \\ \varepsilon_n = \varepsilon_a}} \frac{\psi_n(\boldsymbol{x}_1)\psi_n^+(\boldsymbol{x}_2)}{\varepsilon - \omega - \varepsilon_a + i0}, \tag{56}$$

where we take into account all states with the same energy as the reference state, i.e., also the state with opposite parity but the same total angular momentum as compared to the reference state (pairs of states with the same $|\kappa|$ are energetically degenerate according to Dirac theory).

The evaluation of Eq. (54) proceeds along the integration contour C_M of Mohr [30] for the (complex rather than real) photon energy. It is divided into a low-energy and a high-energy part. The low-energy contour C_L' comprises the interval $\omega \in (\varepsilon_a - i0, -i0)$ below the cut of the photon propagator and the interval $(i0, \varepsilon_a + i0)$ on the upper bank of the cut, with ε_a being the reference-state energy. The high-energy contour C_H' again consists of two intervals, $(\varepsilon_a + i0,\ \varepsilon_a + i\infty)$ and $(\varepsilon_a - i0,\ \varepsilon_a - i\infty)$. Because the low-energy part extends to comparatively high values of $|\omega|$, the radial integrand for each single value of κ becomes highly oscillatory. The behavior of the integrand can only be improved if the full sum over intermediate angular momenta is carried out before the radial integrations. This is already evident from the model example given in Eq. (7.3) of Ref. [31],

$$\frac{\exp(-r[1-\rho])}{r[1-\rho]} = -\sum_{|\kappa|=0}^{\infty} (2|\kappa|+1) j_{|\kappa|}(i\rho r) h_{|\kappa|}^{(1)}(ir), \tag{57}$$

where j is a Bessel function and $h^{(1)}$ is a Hankel function of the first kind ($0 < \rho < 1$). The right-hand side of Eq. (57) involves functions that are highly oscillatory as a function of the radial variable r, but the left-hand side is a simple exponential. This "smoothing" phenomenon after the summation over the intermediate angular momenta is crucial for the evaluation, as it enhances the rate of convergence of the multidimensional SE integrals dramatically. The convergence of the sum over $|\kappa|$ can be further accelerated by the so-called combined nonlinear condensation (CNC) transformation [31]. With maximum values of κ in excess of 10^6 being handled at ease using the CNC transformation, we are able to control the accuracy of the final evaluations. The derivative of Green's function is calculated directly using four-point and (alternatively, for verification) six-point difference schemes. We choose suitable values of the parameters so that the Green's function derivative is calculated to a relative accuracy of 10^{-24}. Additional modifications are necessary in the extreme infrared region of photon energies; here the difference scheme is adjusted so that the boundaries of the integration region are not crossed and sufficient accuracy is retained. A numerical subtraction of all singular terms due to lower-lying atomic states (e.g., the ground state) before doing any integrations over the photon energies and before evaluating the derivative of the Dirac

propagator eliminates a potential further source of numerical loss of significance for the many-potential reducible part.

G. Irreducible part

With reference to Eq. (5), we recall that the irreducible part is given as

$$\Delta E_{\rm ir} = \langle \delta a|\gamma^0 \widetilde{\Sigma}(\varepsilon_a)|a\rangle + \langle a|\gamma^0 \widetilde{\Sigma}(\varepsilon_a)|\delta a\rangle, \qquad (58)$$

with the renormalized SE operator $\widetilde{\Sigma}$ and the perturbed wave function [see Eq. (4)]

$$|\delta a\rangle = \sum_{\substack{n \\ \varepsilon_n \neq \varepsilon_a}} \frac{|n\rangle\langle n|\delta V|a\rangle}{\varepsilon_a - \varepsilon_n}. \qquad (59)$$

We only need the diagonal-in-κ component of the perturbed wave function, because the SE operator is also diagonal in the total angular momentum.

The evaluation of the irreducible part is carried out along the same contour C_M that is used for the many-potential reducible part. Within the high-energy part, Green's function is divided into two parts. The first is a subtraction term which involves a free propagator and an approximate one-potential term [30], which is obtained from the full one-potential term by commuting the Coulomb potential to the left of the electron propagators. The second is the remainder term, which is the difference of the full and the approximate propagator. The subtraction term contains all UV divergences of the irreducible part; these are canceled against the mass counterterm δm. The subtraction term is evaluated in momentum space, in a noncovariant integration scheme adjusted for bound-state calculations, where the spatial components of the photon momentum are integrated out before the photon energy integration.

IV. NUMERICAL RESULTS

Our calculation of the SE correction to the hfs and the g factor of hydrogenlike ions was performed in the Feynman gauge and for a point nucleus. The fine structure constant of $\alpha^{-1} = 137.036$ was used in the calculation. The small deviation of this value from the currently accepted one [19] does not influence the numerical results for the higher-order remainder. An example set of individual contributions to the SE correction to the $1S$ hfs of atomic hydrogen is presented in Table II.

The SE correction to the hfs of an nS state can be represented as

$$\begin{aligned}\Delta E_{nS} = \frac{\alpha}{\pi} E_F(nS)[a_{00} + (Z\alpha)a_{10} \\ + (Z\alpha)^2\{\ln^2[(Z\alpha)^{-2}]a_{22} + \ln[(Z\alpha)^{-2}]a_{21} + a_{20}\} \\ + (Z\alpha)^3 \ln[(Z\alpha)^{-2}]a_{31} + (Z\alpha)^3 F_{nS}(Z\alpha)],\end{aligned} \qquad (60)$$

where $E_F(nS)$ is the nonrelativistic hfs value, and the a_{ij} are coefficients of the $Z\alpha$ expansion with the first index corresponding to the power of $Z\alpha$ and the second corresponding to the power of the logarithm. We have

$$\begin{aligned} a_{00}(nS) &= 1/2, \quad a_{10}(nS) = -8.03259003, \\ a_{22}(nS) &= -2/3, \quad a_{31}(nS) = -13.30741592, \end{aligned} \qquad (61)$$

TABLE II. Individual contributions to the SE correction to the hfs of the $1S$ state of hydrogen, in units $\Delta E/[\alpha/\pi E_F]$. The specific contributions are discussed in Secs. III B ($\Delta E^{(a)}$), III C ($\Delta E^{(0)}_{\rm red}$ and $\Delta E^{(0)}_{\rm ver}$), III D ($\Delta E^{(1)}_{\rm ver}$), III E ($\Delta E^{(2+)}_{\rm ver}$), III F ($\Delta E^{(1+)}_{\rm red}$), and III G ($\Delta E_{\rm ir}$).

$\Delta E_{\rm ir}$	−0.01096549784(5)
$\Delta E^{(0)}_{\rm red}$	8.28956864683
$\Delta E^{(1+)}_{\rm red}$	−3.83854412893(5)
$\Delta E^{(0)}_{\rm ver}$	−5.57958625925
$\Delta E^{(1)}_{\rm ver}$	−1.7835813412(16)
$\Delta E^{(2+)}_{\rm ver}$	3.3612340923(4)
$\Delta E^{(a)}$	−0.00002366906
Total	0.4381018429(16)

$$\begin{aligned} a_{21}(1S) &= -1.334503593, \\ a_{21}(2S) &= 0.317103926, \\ a_{21}(3S) &= 0.921048823, \end{aligned} \qquad (62)$$

$$\begin{aligned} a_{20}(1S) &= 17.12233875, \\ a_{20}(2S) &= 11.90110542, \\ a_{20}(3S) &= 10.41704775, \end{aligned} \qquad (63)$$

see the recent articles [33–35] and references therein for earlier studies. F_{nS} is the higher-order remainder, which we address in our numerical all-order approach. Our numerical results for the SE correction to the hfs of the $1S$, $2S$, and $3S$ states are listed in Table III.

The SE correction to the hfs of an nP_J states is much less studied. Only the leading term of its $Z\alpha$ expansion is known today. The correction, therefore, is written as

$$\Delta E_{nP_J} = E_F(nP_J)\frac{\alpha}{\pi}[a_{00} + (Z\alpha)^2 G_{nP_J}(Z\alpha)], \qquad (64)$$

with G_{nP_J} being the higher-order remainder. The coefficient a_{00} is given by $a_{00}(nP_{1/2}) = 1/4$ and $a_{00}(nP_{3/2}) = -1/8$ [36]. Our numerical results for the SE correction to the hfs of the $2P_{1/2}$ and $2P_{3/2}$ states are listed in Table IV.

The results for the higher-order remainders F_{nS} and G_{nP_J} inferred from our numerical data are plotted in Figs. 2 and 3, respectively. For the $2P_{1/2}$ state, a fit of our results is consistent with the $Z\alpha$ expansion of the form

$$G_{nP_{1/2}}(Z\alpha) = a_{21}\ln[(Z\alpha)^{-2}] + a_{20} + \cdots, \qquad (65)$$

where the value of the logarithmic coefficient is very close to $a_{21}(2P_{1/2}) = -3/2$ and the constant term is about $a_{20}(2P_{1/2}) = 3.5$. For the $2P_{3/2}$ state, the numerical data are consistent with $a_{21}(2P_{3/2}) = 0$. Our results in Table IV are in moderate agreement with those obtained previously in Refs. [13,14] but significantly improve upon them in numerical accuracy. Nevertheless, we disagree with the suggestion [13] about the possible presence of the squared logarithm in the $Z\alpha$ expansion (65) for the $2P_{1/2}$ state. A more careful investigation of the analytic structure of the higher-order terms is performed in the follow-up paper [37].

TABLE III. SE correction to the hfs of nS states of hydrogenlike ions. $\delta E_{nS} = \Delta E_{nS}/[\alpha/\pi E_F(nS)]$ and F_{nS} is the higher-order remainder defined by Eq. (60).

$1S$	Z	δE_{1S}	$F_{1S}(Z\alpha)$
	1	0.4381018429(16)	−13.8308(43)
	2	0.373467600(3)	−14.1170(9)
	3	0.307583838(4)	−14.4121(3)
	4	0.241005731(5)	−14.6962(2)
	5	0.174026212(7)	−14.9673(2)
	6	0.106815805(11)	−15.2264(1)
	7	0.03947649(2)	−15.4752(1)
	8	−0.02793233(2)	−15.7156(1)
	9	−0.09537946(3)	−15.9487(1)
	10	−0.16285352(4)	−16.1762(1)
	11	−0.23035739(4)	−16.3990(1)
	12	−0.29790470(4)	−16.6181(1)
$2S$	Z	δE_{2S}	$F_{2S}(Z\alpha)$
	1	0.438692275(3)	−6.1205(85)
	2	0.375352042(3)	−6.9126(11)
	3	0.311203194(5)	−7.5833(5)
	4	0.246665425(7)	−8.1697(3)
	5	0.181938687(9)	−8.7069(2)
	6	0.117123392(13)	−9.1973(2)
	7	0.05226463(2)	−9.6546(1)
	8	−0.01262594(2)	−10.0859(1)
	9	−0.07755851(3)	−10.4964(1)
	10	−0.14255836(3)	−10.8901(1)
	11	−0.20766159(3)	−11.2701(1)
	12	−0.27291238(4)	−11.6390(1)
$3S$	Z	δE_{3S}	$F_{3S}(Z\alpha)$
	1	0.43893143(3)	−1.727(69)
	2	0.37613687(3)	−2.6138(90)
	3	0.31274865(3)	−3.3530(27)
	4	0.24914165(3)	−3.9994(12)
	5	0.18548734(3)	−4.5806(7)
	6	0.12186545(3)	−5.1133(4)
	7	0.05830586(3)	−5.6092(2)
	8	−0.00519144(3)	−6.0757(1)
	9	−0.06864589(3)	−6.5189(1)
	10	−0.13209008(3)	−6.9430(1)
	11	−0.19556594(4)	−7.3515(1)
	12	−0.25912227(5)	−7.7473(1)

The SE correction to the bound-electron g factor of an nS state can be represented as

$$\Delta g_{nS} = \frac{\alpha}{\pi}\left[1 + \frac{(Z\alpha)^2}{n^2} b_{20} + \frac{(Z\alpha)^4}{n^3}\{\ln[(Z\alpha)^{-2}]b_{41} + b_{40}\} + \frac{(Z\alpha)^5}{n^3} H_{nS}(Z\alpha)\right], \tag{66}$$

where the b_{ij} are known coefficients of the $Z\alpha$ expansion:

$$\begin{aligned} b_{20}(nS) &= \tfrac{1}{6}, \qquad b_{41}(nS) = \tfrac{32}{9}, \\ b_{40}(1S) &= -10.23652432, \\ b_{40}(2S) &= -10.70771560, \\ b_{40}(3S) &= -11.52963397, \end{aligned} \tag{67}$$

TABLE IV. SE correction to the hfs of $2P_J$ states of hydrogenlike ions. $\delta E_{nP_J} = \Delta E_{nP_J}/[\alpha/\pi E_F(nP_J)]$, and G_{nP_J} is the higher-order remainder defined by Eq. (64).

$2P_{1/2}$	Z	$\delta E_{2P_{1/2}}$	$G_{2P_{1/2}}(Z\alpha)$
	1	0.249397018(5)	−11.323321(86)
		0.2487(5)[a]	
	2	0.248016543(5)	−9.311768(25)
	3	0.246087170(7)	−8.164278(14)
	4	0.243719931(7)	−7.370786(9)
	5	0.240985405(8)	−6.771355(6)
		0.2397[a]	
	6	0.237932761(8)	−6.294696(4)
	7	0.234597810(8)	−5.902768(3)
	8	0.231007222(8)	−5.572857(2)
	9	0.227180996(8)	−5.290309(2)
	10	0.223134035(8)	−5.045123(2)
		0.2202[a]	
	11	0.218877214(8)	−4.830170(1)
	12	0.214418110(9)	−4.640191(1)
$2P_{3/2}$	Z	$\delta E_{2P_{3/2}}$	$G_{2P_{3/2}}(Z\alpha)$
	1	−0.12499329(1)	0.12609(18)
		−0.1254[b]	
	2	−0.12498309(1)	0.079405(55)
	3	−0.12498458(2)	0.032176(39)
	4	−0.12501321(2)	−0.015499(29)
	5	−0.12508457(3)	−0.063528(21)
		−0.1255[b]	
	6	−0.12521458(3)	−0.111933(16)
	7	−0.12541922(3)	−0.160663(12)
	8	−0.12571467(3)	−0.209698(9)
	9	−0.12611728(3)	−0.259028(7)
	10	−0.12664357(3)	−0.308643(5)
		−0.1271[b]	
	11	−0.12731021(3)	−0.358538(5)
	12	−0.12813408(3)	−0.408711(4)

[a]Ref. [13].
[b]Ref. [14].

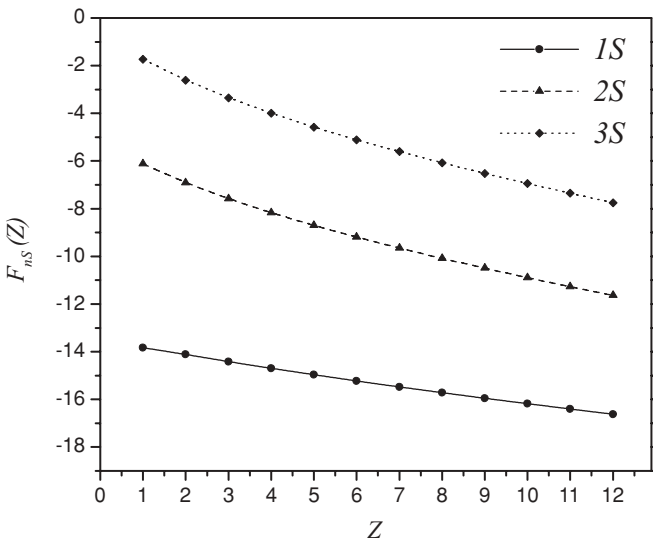

FIG. 2. The higher-order remainder $F_{nS}(Z\alpha)$ for the SE correction to the hfs of the $1S$, $2S$, and $3S$ states.

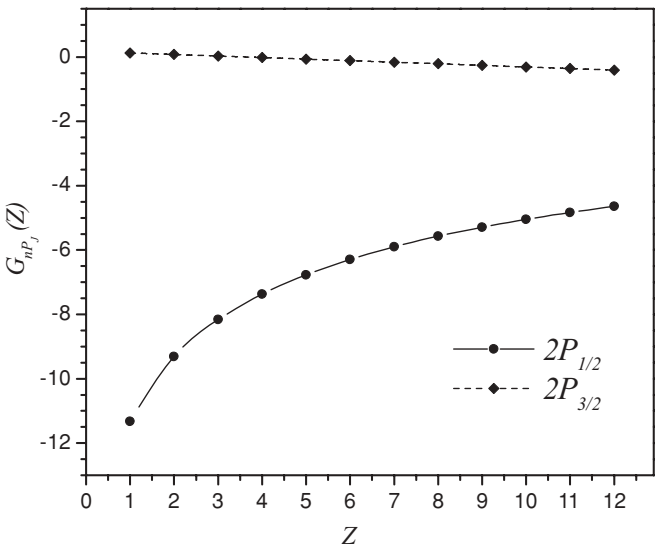

FIG. 3. The higher-order remainder $G_{nP_J}(Z\alpha)$ for the SE correction to the hfs of the $2P_{1/2}$ and $2P_{3/2}$ states.

see Ref. [38] and references therein. H_{nS} is the remainder incorporating all higher-order contributions. It is remarkable that the higher-order remainder H_{nS} enters in the relative order $(Z\alpha)^5$ rather than in the relative order $(Z\alpha)^3$, as in the case of the hfs. This means that cancellations in extracting the remainder from numerical results for $Z = 1$ are larger for the g factor than for the hfs by four orders of magnitude.

Our numerical results for the SE correction to the g factor of the electron $1S$, $2S$, and $3S$ states of light hydrogenlike ions are presented in Table V. We observe that the higher-order remainder behaves very similarly for all nS states studied, the $2S$ remainder being just about 2% larger than that for the $1S$ states, and the $3S$ and $2S$ remainders being equal within the numerical uncertainty. The accuracy of the direct numerical determination of the $1S$ remainder for $Z = 1$ and $Z = 2$ can easily be increased by extrapolating values obtained for higher values of Z. An extrapolation yields the improved results $H_{1S}(1\alpha) = 23.39(80)$ and $H_{1S}(2\alpha) = 23.03(44)$. Improved values of the higher-order remainder for the $2S$ and $3S$ states are most easily obtained by scaling the $1S$ remainder. The trend of the higher-order remainder for low Z is consistent with a numerically large, n-independent coefficient b_{50} in Eq. (66).

For the P_J states, the bound-electron g factor is studied less thoroughly than for the S states. The leading term of its $Z\alpha$ expansion is due to the electron anomalous magnetic moment (AMM) and is immediately obtained for a general state as [39]

$$b_{00} = \frac{1 - 2\kappa}{4j(j+1)}, \tag{68}$$

where κ is the Dirac quantum number and j is the total angular momentum of the electron state. For the P states, the explicit results are $b_{00}(nP_{1/2}) = -1/3$ and $b_{00}(nP_{3/2}) = 1/3$.

The next-order term, b_{20}, consists of two parts: one induced by the electron AMM, and the other by the emission and absorption of virtual photons of low energy (commensurate with the electron binding energy). A simple calculation of the first part gives [39] $b_{20}(nP_{1/2}, \text{AMM}) = -1/2$ and $b_{20}(nP_{3/2}, \text{AMM}) = 1/10$. The second part is nonvanishing for states with $l \neq 0$ only and is more complicated. Its general expression is known [40,41] but the only numerical result available for hydrogenic atoms is the estimate made in Ref. [42], which disagrees with our numerical values both in the sign and the magnitude. Commenting on this fact, we note that the estimate is based on a rather crude approximation. Namely, the sum over the entire discrete and continuous spectrum of virtual states was replaced by the contribution of the lowest 12 discrete bound states only. We argue that such approximation might be inapplicable for the problem in hand. The reason is that, e.g., for the Bethe logarithm (which is also a contribution induced by the low-energy photons), the dominant contribution originates from the continuum spectrum [43] so that such an approximation is clearly inadequate.

TABLE V. SE correction to the g factor of nS states of hydrogenlike ions, in ppm. H_{nS} is the higher-order remainder.

$1S$	Z	Δg_{1S}	$H_{1S}(Z\alpha)$
	1	2322.840230(2)	19(3)
	2	2322.904037(4)	23.3(2.6)
	3	2323.014295(8)	22.88(70)
	4	2323.175525(14)	22.58(29)
	5	2323.39298(2)	22.36(15)
	6	2323.67243(3)	22.18(9)
	7	2324.02001(5)	22.02(6)
	8	2324.44213(7)	21.87(4)
	9	2324.94538(8)	21.71(3)
	10	2325.53651(10)	21.57(2)
	11	2326.22235(13)	21.42(2)
	12	2327.00983(12)	21.28(1)
$2S$	Z	Δg_{2S}	$H_{2S}(Z\alpha)$
	1	2322.824624(2)	
	2	2322.840323(8)	
	3	2322.86696(2)	19(11)
	4	2322.90509(3)	22.1(4.7)
	5	2322.95533(5)	22.5(2.4)
	6	2323.01836(6)	22.5(1.3)
	7	2323.09490(8)	22.43(74)
	8	2323.18571(8)	22.31(42)
	9	2323.29154(9)	22.18(24)
	10	2323.41319(9)	22.05(15)
	11	2323.55142(11)	21.92(11)
	12	2323.70704(12)	21.79(8)
$3S$	Z	Δg_{3S}	$H_{3S}(Z\alpha)$
	1	2322.821746(7)	
	2	2322.828684(10)	
	3	2322.84038(2)	
	4	2322.85698(3)	19(18)
	5	2322.87866(5)	20.7(8.4)
	6	2322.90560(6)	21.5(4.6)
	7	2322.93798(9)	21.8(2.9)
	8	2322.97600(12)	22.0(2.0)
	9	2323.0198(2)	22.0(1.4)
	10	2323.0697(2)	22.0(1.0)
	11	2323.1258(2)	21.89(77)
	12	2323.1882(3)	21.81(59)

TABLE VI. SE correction to the g factor of $2P_J$ states of hydrogenlike ions, in ppm. I_{nP_J} is the higher-order remainder.

$2P_{1/2}$	Z	$\Delta g_{2P_{1/2}}$	$I_{2P_{1/2}}(Z\alpha)$
	1	−774.258151(3)	0.121258(21)
	2	−774.212929(11)	0.121715(22)
	3	−774.13687(2)	0.122414(19)
	4	−774.02917(3)	0.123280(14)
	5	−773.88876(3)	0.124305(10)
	6	−773.71442(3)	0.125473(7)
	7	−773.50460(3)	0.126803(5)
	8	−773.25838(3)	0.128186(4)
	9	−772.97356(3)	0.129711(2)
	10	−772.64862(3)	0.131336(2)
	11	−772.28175(4)	0.133054(3)
	12	−771.87108(8)	0.134858(5)
$2P_{3/2}$	Z	$\Delta g_{2P_{3/2}}$	$I_{2P_{3/2}}(Z\alpha)$
	1	774.291470(3)	0.148104(21)
	2	774.346522(12)	0.148294(24)
	3	774.43854(3)	0.148567(24)
	4	774.56774(4)	0.148851(22)
	5	774.73495(6)	0.149338(18)
	6	774.94028(6)	0.149816(14)
	7	775.18442(6)	0.150350(11)
	8	775.46799(6)	0.150933(7)
	9	775.79167(5)	0.151561(4)
	10	776.15615(5)	0.152231(4)
	11	776.56218(6)	0.152940(4)
	12	777.01055(6)	0.153685(4)

Since the $(Z\alpha)^2$ term is not presently known analytically, we define the higher-order remainder for the P_J states as

$$\Delta g_{nP_J} = \frac{\alpha}{\pi}[b_{00} + (Z\alpha)^2 I_{nP_J}(Z\alpha)]. \tag{69}$$

Our numerical results for the SE correction to the g factor of the electron $2P_{1/2}$ and $2P_{3/2}$ states of light hydrogenlike ions are listed in Table VI. The corresponding higher-order remainder function is plotted in Fig. 4.

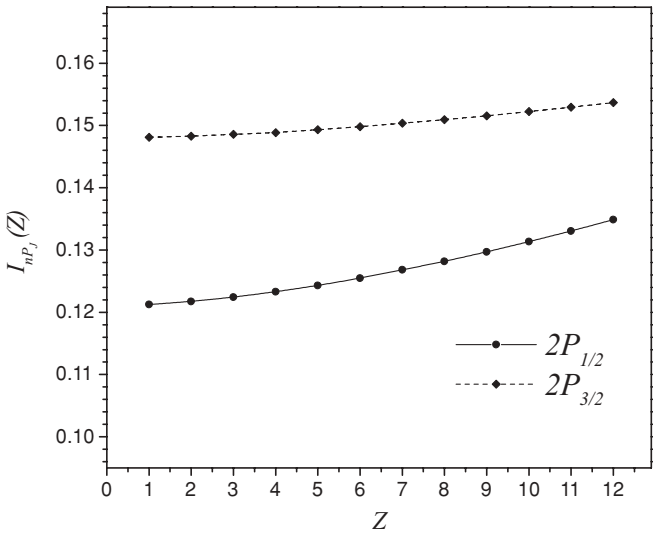

FIG. 4. The higher-order remainder for the SE correction to the g factor of the $2P_{1/2}$ and $2P_{3/2}$ states.

V. CONCLUSIONS

We have discussed, in detail, a numerical evaluation, nonperturbative in the binding Coulomb field, of the self-energy correction to the hyperfine splitting and of the self-energy correction to the g factor in hydrogenlike ions with low nuclear charge number $Z = 1, \ldots, 12$. We consider the ground state, the $2S$ and $3S$ excited states, and the $2P_{1/2}$ and $2P_{3/2}$ states. The value of $\alpha^{-1} = 137.036$ is employed in all calculations. At the level of precision we are operating at, the final results for the self-energy corrections depend very sensitively on the precise value being employed. However, the main dependence on the value of α is accounted for by the analytically known lower-order terms. Thus, the results for the remainder functions $F_{nS}(Z\alpha)$, $G_{nP_J}(Z\alpha)$, $H_{nS}(Z\alpha)$, and $I_{nP_J}(Z\alpha)$ as given in Tables III, IV, V, and VI, respectively, are not influenced by the value of α employed. Even if a value of α which differs from $\alpha^{-1} = 137.036$ on the level 10^{-7} were employed, then the values of the remainder functions would not change: their main uncertainty is due to limits of convergence of the integrals that constitute the nonperturbative self-energy corrections, as described in the preceding sections of this article.

The organization of our calculation is described in Sec. III. We consider separately the reference-state contribution to the reducible and the vertex part (Sec. III B) and the zero-potential contribution to the vertex and to the reducible part (Sec. III C). The one-potential and many-potential vertex parts, which represent the most challenging part of the calculation, are discussed in Secs. III D and III E. The many-potential reducible part and the irreducible part conclude the discussion of our computational method (Secs. III F and III G). Numerical calculations were carried out on the parallel computing environments of MPI Heidelberg and MST Rolla.

It is instructive to compare the numerical results obtained (Tables III–VI) with analytic results from the $Z\alpha$ expansion. The analytic parametrization of the self-energy correction to the hyperfine splitting according to Eq. (60) entails both logarithmic and nonlogarithmic corrections. Our numerical results for the scaled self-energy correction δE_n to the hyperfine splitting and for the nonperturbative remainder function $F_{nS}(Z\alpha)$ are given in Table III for S states. A plot of the data (see Fig. 2) indicates that the higher-order remainders $F_{nS}(Z\alpha)$, for $Z \to 0$, may converge toward an a_{30} coefficient which is significantly dependent on the principal quantum number.

The scaled self-energy correction δE_{nP_J} for $2P_{1/2}$ and $2P_{3/2}$ states is analyzed in Table IV. A plot of the data (see Fig. 3) aids in a comparison with an analytic model for the correction, given in Eq. (65). The nonperturbative remainder $G_{nP_J}(Z\alpha)$ for the hfs of P states is seen to be well represented by an analytic model of the form $\{a_{21}\ln[(Z\alpha)^{-2}] + a_{20} + \cdots\}$, where a fit to the numerical data indicates that $a_{21}(2P_{1/2}) = -3/2$ and that $a_{21}(2P_{3/2}) = 0$. It has been suggested in Ref. [13] that a "double" (squared) logarithm in the $Z\alpha$ expansion could be present for low nuclear charge; the latter would correspond to a nonvanishing a_{22} coefficient for P states. Our numerical results

in Table IV do not contradict those of Ref. [13] on the level of numerical accuracy obtained in the cited reference. However, we cannot confirm the presence of such a double-logarithmic correction (see also [37]).

A large number of analytic terms are known for the self-energy correction to the g factor for S states [see Eq. (66)]. The higher-order remainder $H_{nS}(Z\alpha)$ for the g factor of S states is thus "separated" from the leading-order effect by about ten orders of magnitude for $Z = 1$. Thus, although our direct numerical evaluation of the self-energy correction for the ground state at $Z = 1$ is precise [$\Delta g_{1S} = 2322.840230(2) \times 10^{-6}$ at $Z = 1$], we can only infer the higher-order remainder $H_{1S}(Z\alpha)$ at $Z = 1$ to about $\pm 10\%$: the result after the subtraction of lower-order terms is $H_{1S}(1\alpha) = 19(3)$. By extrapolation of more accurate data for the remainder obtained from higher values of the nuclear charge, we can obtain the improved results $H_{1S}(1\alpha) = 23.39(80)$ and $H_{1S}(2\alpha) = 23.03(44)$. The remainder functions at very low Z appear to depend only very slightly on the principal quantum number; they are consistent with $H_{nS}(Z\alpha)$ approaching an n-independent coefficient b_{50} as $Z \to 0$.

For the g factor of P states, only the leading coefficient b_{00} is known from the $Z\alpha$ expansion [see Eq. (69)]. The self-energy remainder function $I_{nP_J}(Z\alpha)$ for the g factor of P states can be inferred from our numerical data in Table VI after subtraction of the leading analytic term as given in Eq. (69). The numerical data for P states are consistent with the functions $I_{nP_J}(Z\alpha)$ tending toward a constant for $Z \to 0$. A plot of the data in Fig. 4 confirms this trend.

To conclude, we have performed an all-order (in $Z\alpha$) calculation of the self-energy correction to hyperfine splitting and g factor in hydrogenlike ions with low nuclear charge numbers. The calculation is accurate enough to infer higher-order remainder terms without any additional extrapolation, by a simple subtraction of the known terms in the $Z\alpha$ expansion. We improve the numerical accuracy by several orders of magnitude over that of previous evaluations; this leads to improved theoretical predictions for all QED effects considered in this article.

ACKNOWLEDGMENTS

Enlightening discussions with K. Pachucki on the g factor of P states are gratefully acknowledged. V.A.Y. was supported by DFG (Grant No. 436 RUS 113/853/0-1), RFBR (Grant No. 06-02-04007), and the foundation "Dynasty." U.D.J. was supported by the National Science Foundation (Grant PHY-80555454) as well as a Precision Measurement Grant from the National Institute of Standards and Technology.

APPENDIX: ANGULAR INTEGRATIONS IN MOMENTUM SPACE

In this section we demonstrate how to perform the integration over the angular variables in momentum space. The problem in hand can be formulated as follows. The general expression of the form

$$\int d\hat{\boldsymbol{p}}_1 d\hat{\boldsymbol{p}}_2 F(p_{1r}, p_{2r}, \xi) A(\hat{\boldsymbol{p}}_1) B(\hat{\boldsymbol{p}}_2), \tag{A1}$$

where F, A, and B are some arbitrary functions and $\xi = \hat{\boldsymbol{p}}_1 \cdot \hat{\boldsymbol{p}}_2$, needs to be integrated over all angular variables except for ξ, i.e., to be reduced to the form

$$\int_{-1}^{1} d\xi F(p_{1r}, p_{2r}, \xi) X(A, B; \xi). \tag{A2}$$

In order to write a general expression for the function $X(\xi)$ in terms of A and B, we use the standard decomposition of the function F in terms of the spherical harmonics Y_{lm},

$$F(p_{1r}, p_{2r}, \xi) = 2\pi \sum_{lm} Y^*_{lm}(\hat{\boldsymbol{p}}_1) Y_{lm}(\hat{\boldsymbol{p}}_2) \times \int_{-1}^{1} d\xi F(p_{1r}, p_{2r}, \xi) P_l(\xi), \tag{A3}$$

where P_l are the Legendre polynomials. From this, we immediately have

$$X(A, B; \xi) = 2\pi \sum_{l=0}^{\infty} P_l(\xi) \sum_{m=-l}^{l} \left[\int d\hat{\boldsymbol{p}}_1 A(\hat{\boldsymbol{p}}_1) Y^*_{lm}(\hat{\boldsymbol{p}}_1) \right] \times \left[\int d\hat{\boldsymbol{p}}_2 B(\hat{\boldsymbol{p}}_2) Y_{lm}(\hat{\boldsymbol{p}}_2) \right]. \tag{A4}$$

This general formula greatly simplifies when one of the functions (say, B) is unity or the identity function, i.e., $B(\hat{\boldsymbol{p}}_2) = \hat{\boldsymbol{p}}_2$. When B is unity, only the term with $l = 0$ contributes, and we have

$$X(A, 1; \xi) = 2\pi \int d\hat{\boldsymbol{p}} A(\hat{\boldsymbol{p}}). \tag{A5}$$

When $B = \mathrm{id}$,

$$X(A, \mathrm{id}; \xi) = 2\pi\xi \int d\hat{\boldsymbol{p}} \hat{\boldsymbol{p}} A(\hat{\boldsymbol{p}}). \tag{A6}$$

In more complicated cases with $B = \hat{\boldsymbol{p}}_i \hat{\boldsymbol{p}}_k \ldots$, formulas for X can be in principle obtained by using the Racah algebra. Alternatively, one can observe [from Eq. (A4)] that X is a combination of the Legendre polynomials with some coefficients. It is straightforward to find the coefficients by performing integrations in Eq. (A4) analytically for each particular case (where advantage may be taken of computer algebra).

In the present work, we need angular integrals of three types, K_1, K_2, and K_3, defined as ($\mu = 1/2$)

$$\frac{3i}{4\pi} \int d\hat{\boldsymbol{p}}_1 d\hat{\boldsymbol{p}}_2 F(p_{1r}, p_{2r}, \xi) \chi^\dagger_{\kappa,\mu}(\hat{\boldsymbol{p}}_1) [\hat{\boldsymbol{p}}_1 \times \boldsymbol{\sigma}]_z \chi_{-\kappa,\mu}(\hat{\boldsymbol{p}}_2) = \int_{-1}^{1} d\xi F(p_{1r}, p_{2r}, \xi) K_1(\kappa), \tag{A7a}$$

$$\frac{3i}{4\pi} \int d\hat{\boldsymbol{p}}_1 d\hat{\boldsymbol{p}}_2 F(p_{1r}, p_{2r}, \xi) \chi^\dagger_{\kappa,\mu}(\hat{\boldsymbol{p}}_1) [\hat{\boldsymbol{p}}_2 \times \boldsymbol{\sigma}]_z \chi_{-\kappa,\mu}(\hat{\boldsymbol{p}}_2) = \int_{-1}^{1} d\xi F(p_{1r}, p_{2r}, \xi) K'_1(\kappa), \tag{A7b}$$

$$\frac{3i}{4\pi} \int d\hat{\boldsymbol{p}}_1 d\hat{\boldsymbol{p}}_2 F(p_{1r}, p_{2r}, \xi) \chi^\dagger_{\kappa,\mu}(\hat{\boldsymbol{p}}_1) [\hat{\boldsymbol{p}}_1 \times \hat{\boldsymbol{p}}_2]_z \chi_{\kappa,\mu}(\hat{\boldsymbol{p}}_2) = \int_{-1}^{1} d\xi F(p_{1r}, p_{2r}, \xi) K_2(\kappa), \tag{A7c}$$

$$\frac{3i}{4\pi} \int d\hat{\boldsymbol{p}}_1 d\hat{\boldsymbol{p}}_2 F(p_{1r}, p_{2r}, \xi) \chi^\dagger_{\kappa,\mu}(\hat{\boldsymbol{p}}_1) i\boldsymbol{\sigma}_z \chi_{\kappa,\mu}(\hat{\boldsymbol{p}}_2) = \int_{-1}^{1} d\xi F(p_{1r}, p_{2r}, \xi) K_3(\kappa). \tag{A7d}$$

Using the technique described above, we obtain the following results for the basic angular integrals:

$$K_1(\kappa) = \begin{cases} -\xi, & \kappa = -1, \\ 1, & \kappa = 1, \\ \frac{1}{5}(1-3\xi^2), & \kappa = -2, \\ \frac{2}{5}\xi, & \kappa = 2, \end{cases} \tag{A8a}$$

$$K_1'(\kappa) = \begin{cases} -1, & \kappa = -1, \\ \xi, & \kappa = 1, \\ -\frac{2}{5}\xi, & \kappa = -2, \\ -\frac{1}{5}(1-3\xi^2), & \kappa = 2, \end{cases} \tag{A8b}$$

as well as

$$K_2(\kappa) = \begin{cases} 0, & \kappa = -1, \\ -\frac{1}{2}(1-\xi^2), & \kappa = 1, \\ -\frac{1}{4}(1-\xi^2), & \kappa = -2, \\ -\frac{9}{20}\xi(1-\xi^2), & \kappa = 2, \end{cases} \tag{A8c}$$

$$K_3(\kappa) = \begin{cases} -\frac{3}{2}, & \kappa = -1, \\ \frac{1}{2}\xi, & \kappa = 1, \\ -\frac{1}{2}\xi, & \kappa = -2, \\ -\frac{3}{20}(1-3\xi^2), & \kappa = 2. \end{cases} \tag{A8d}$$

[1] H. Persson, S. M. Schneider, W. Greiner, G. Soff, and I. Lindgren, Phys. Rev. Lett. **76**, 1433 (1996).

[2] V. M. Shabaev and V. A. Yerokhin, Pis'ma Zh. Eksp. Teor. Fiz. **63**, 309 (1996) [JETP Lett. **63**, 316 (1996)].

[3] S. A. Blundell, K. T. Cheng, and J. Sapirstein, Phys. Rev. A **55**, 1857 (1997).

[4] S. A. Blundell, K. T. Cheng, and J. Sapirstein, Phys. Rev. Lett. **78**, 4914 (1997).

[5] H. Persson, S. Salomonson, P. Sunnergren, and I. Lindgren, Phys. Rev. A **56**, R2499 (1997).

[6] P. Sunnergren, H. Persson, S. Salomonson, S. M. Schneider, I. Lindgren, and G. Soff, Phys. Rev. A **58**, 1055 (1998).

[7] T. Beier, I. Lindgren, H. Persson, S. Salomonson, P. Sunnergren, H. Häffner, and N. Hermanspahn, Phys. Rev. A **62**, 032510 (2000).

[8] V. A. Yerokhin and V. M. Shabaev, Phys. Rev. A **64**, 012506 (2001).

[9] J. Sapirstein and K. T. Cheng, Phys. Rev. A **63**, 032506 (2001).

[10] V. A. Yerokhin, P. Indelicato, and V. M. Shabaev, Phys. Rev. Lett. **89**, 143001 (2002).

[11] V. A. Yerokhin, P. Indelicato, and V. M. Shabaev, Phys. Rev. A **69**, 052503 (2004).

[12] V. A. Yerokhin, A. N. Artemyev, V. M. Shabaev, and G. Plunien, Phys. Rev. A **72**, 052510 (2005).

[13] J. Sapirstein and K. T. Cheng, Phys. Rev. A **74**, 042513 (2006).

[14] J. Sapirstein and K. T. Cheng, Phys. Rev. A **78**, 022515 (2008).

[15] H. A. Schluesser, E. N. Fortson, and H. G. Dehmelt, Phys. Rev. **187**, 5 (1969); Phys. Rev. A **2**, 1612(E) (1970).

[16] M. H. Prior and E. C. Wang, Phys. Rev. A **16**, 6 (1977).

[17] S. G. Karshenboim and V. G. Ivanov, Can. J. Phys. **83**, 1063 (2005).

[18] V. A. Yerokhin and U. D. Jentschura, Phys. Rev. Lett. **100**, 163001 (2008).

[19] P. J. Mohr, B. N. Taylor, and D. B. Newell, Rev. Mod. Phys. **80**, 633 (2008).

[20] W. Quint, B. Nikoobakht, and U. D. Jentschura, Pis'ma Zh. Eksp. Teor. Fiz. **87**, 36 (2008) [JETP Lett. **87**, 30 (2008)].

[21] V. M. Shabaev, Phys. Rep. **356**, 119 (2002).

[22] U. D. Jentschura, P. J. Mohr, and G. Soff, Phys. Rev. Lett. **82**, 53 (1999).

[23] U. D. Jentschura, P. J. Mohr, and G. Soff, Phys. Rev. A **63**, 042512 (2001).

[24] V. M. Shabaev, J. Phys. B **24**, 4479 (1991).

[25] V. Shabaev, in *Precision Physics of Simple Atomic Systems*, edited by S. G. Karshenboim and V. B. Smirnov (Springer, Berlin, 2003), p. 97.

[26] V. A. Yerokhin, A. N. Artemyev, T. Beier, G. Plunien, V. M. Shabaev, and G. Soff, Phys. Rev. A **60**, 3522 (1999).

[27] C. L. Pekeris, Phys. Rev. **112**, 1649 (1958).

[28] V. A. Yerokhin, P. Indelicato, and V. M. Shabaev, Eur. Phys. J. D **25**, 203 (2003).

[29] R. R. Lewis, Phys. Rev. **102**, 537 (1956).

[30] P. J. Mohr, Ann. Phys. (NY) **88**, 26 (1974).

[31] U. D. Jentschura, P. J. Mohr, G. Soff, and E. J. Weniger, Comput. Phys. Commun. **116**, 28 (1999).

[32] V. A. Yerokhin and V. M. Shabaev, Phys. Rev. A **60**, 800 (1999).

[33] K. Pachucki, Phys. Rev. A **54**, 1994 (1996).

[34] M. Nio and T. Kinoshita, Phys. Rev. D **55**, 7267 (1997).

[35] S. G. Karshenboim and V. G. Ivanov, Eur. Phys. J. D **19**, 13 (2002).

[36] S. J. Brodsky and R. G. Parsons, Phys. Rev. **176**, 423 (1968).

[37] U. D. Jentschura and V. A. Yerokhin (in press).

[38] K. Pachucki, U. D. Jentschura, and V. A. Yerokhin, Phys. Rev. Lett. **93**, 150401 (2004); **94**, 229902(E) (2005).

[39] H. Grotch and R. Kashuba, Phys. Rev. A **7**, 78 (1973).

[40] H. Grotch and R. A. Hegstrom, Phys. Rev. A **8**, 2771 (1973).

[41] K. Pachucki, Phys. Rev. A **69**, 052502 (2004).

[42] J. Calmet, H. Grotch, and D. A. Owen, Phys. Rev. A **17**, 1218 (1978). This Comment estimates the low-energy contribution to the g factor of the $2P$ states of hydrogen to be $\delta g_L(2P) = -0.24\alpha^3$. In order to convert this value to the g_J factor addressed in the present investigation, it should be multiplied by $[j(j+1)+l(l+1)-s(s+1)]/[2j(j+1)]$. In units of the coefficient b_{20} defined by Eq. (66), this estimate corresponds to $\delta b_{20}(2P_{1/2}) = -4.0$ and $\delta b_{20}(2P_{3/2}) = -2.0$, in strong disagreement with our numerical results.

[43] G. W. F. Drake and S. P. Goldman, Can. J. Phys. **77**, 835 (1999).